ACS APPLIED MATERIALS & INTERFACES

Research Article

www.acsami.org

Preparation and Characterization of Molecularly Homogeneous Silica–Titania Film by Sol–Gel Process with Different Synthetic Strategies

Hsueh-Shih Chen,*[,†] Sheng-Hsin Huang,[†] and Tsong-Pyng Perng*[,†,‡]

[†]Department of Materials Science and Engineering, National Tsing Hua University, Hsinchu 300, Taiwan

[‡]Department of Chemical Engineering and Materials Science, Yuan Ze University, Chungli 320, Taiwan

Supporting Information

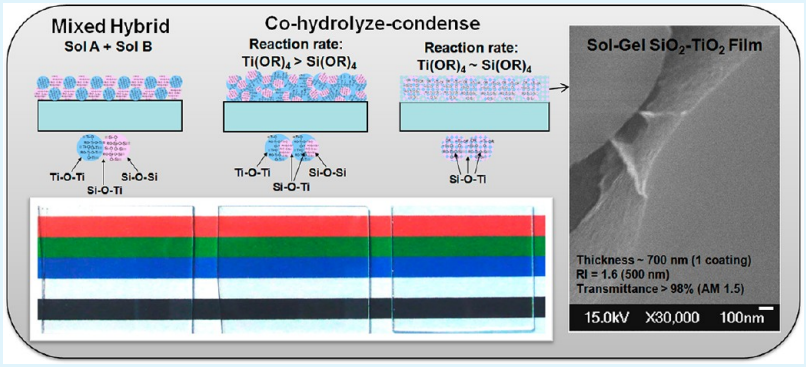

ABSTRACT: Three silica–titania thin films with various degrees of molecular homogeneity were synthesized by the sol–gel process with the same precursor formula but different reaction paths. The dried films prepared by a single spin-coating process have a thickness of 500–700 nm and displayed no cracks or pin holes. The transmittances and refractive indices of the samples are >97.8% in the range of 350–1800 nm and 1.62–1.65 at 500 nm, respectively. The in-plane and out-of-plane chemical homogeneities of the films were analyzed by X-ray photoelectron spectroscopy and Auger electron spectroscopy, respectively. For the film with the highest degree of homogeneity, the deviations of O, Si, and Ti atomic contents in both in-plane and out-of-plane directions are less than 1.5%, indicating that the film is highly molecularly homogeneous. It also possesses the highest transparency and the lowest refractive index among the three samples.

KEYWORDS: *antireflective, silica–titania, sol–gel, SiO_2, TiO_2, transparent film*

1. INTRODUCTION

The advantages of chemical solution deposition of materials are flexible processing, low cost, and good control over the morphology.[1] Among the solution-based processes, the sol–gel method is well-suited for preparing both simple and complex metal oxides as the gel network can spatially trap different ions in the molecular dimension that greatly reduces their diffusion distance and thus improves the phase homogeneity of the metal oxides in a post alloying process. The sol–gel method is capable of preparing materials with a wide variety of morphologies and grain sizes through adjusting the precursor solution chemistry. These structural and operational flexibilities largely extend its practicability to various applications such as anticorrosive film,[2] antireflective layer,[3] biocompatible coating,[4] electrical insulation coating,[5] and photocatalyst.[6]

Silica–titania transparent film prepared from the sol–gel process is thermally and chemically stable. So it has been considered as a protective coating for large scale optical and biological applications.[7] In order to achieve an optical grade, transparent films require molecular homogeneity in composition, dense microstructure without cavities, and highly smooth surface. However, for sol–gel-derived multicomponent oxides, such as SiO_2–TiO_2, the phase homogeneity is generally low because of much faster reaction rate of Ti precursors (e.g., alkoxides) compared to that of Si ones. Yoldas suggested that the phase homogeneity of SiO_2–TiO_2 could be improved by mixing prehydrolyzed Si alkoxides with Ti alkoxides, which produced Si–O–Ti bonds.[8] Other strategies to improve the phase homogeneity were also reported, for example, stabilization of Ti alkoxides by modifiers,[9] varying size of alkoxy groups of Si and Ti,[10] nonhydrolytic sol–gel process,[11] and so on. The phase homogeneity of silica–titania hybrid can be judged by examining the existence of heterometal oxides Si–O–Ti bonds using nuclear magnetic resonance (NMR) spectroscopy such as ^{29}Si or ^{17}O NMR.[12−16] From NMR studies, it was found that the content of the Si–O–Ti bonds in silica–titania hybrid was

Received: June 20, 2012
Accepted: August 30, 2012
Published: August 30, 2012

generally low due to the hydrolytic stability of the Si−O−Ti bonds.[14,15] This instability of the Si−O−Ti bonds therefore causes heterogeneity of the silica−titania hybrid.[17]

Although NMR has been widely used to study the hydrolysis−condensation and homogeneity of silica−titania hybrid in the liquid phase or in the powder form, there were very few reports for solid-state silica−titania thin film regarding its molecular homogeneity and microstructure. Since the thin film processing such as coating and annealing significantly changes the morphology and the composition of silica−titania materials, the phase homogeneity and the microstructure of such kind of thin solid films are different from those in the liquid phase or in the powder form. In this paper, we synthesized three silica−titania thin solid films with different homogeneity and analyzed their in-plane and out-of-plane compositions and phase homogeneities by X-ray photoelectron spectroscopy and Augar electron spectroscopy.

2. EXPERIMENTAL SECTION

Titanium isopropoxide (TTIP, $Ti(OC_3H_7)_4$), 1-propanol, pentane-2,4-dione (acetylacetone, acac), tetraethoxysilane (TEOS, $Si(OC_2H_5)_4$), and absolute ethanol were used as received. The titania precursor solution was prepared by mixing 3.1 mmol TTIP with 33.3 mmol 1-propanol. The silica precursor solution was prepared by mixing 8.6 mmol TEOS with 103.2 mmol ethanol. Acac was used as a stabilizer similar to acetic acid.[18] Hydrolysis was carried out by mixing precursor solutions with deionized water. The R_w (H_2O/TTIP) was ~2. The molar ratio of Ti to Si was 0.36. The pH values of samples were adjusted smaller than 4.

Three sols were prepared by three different reaction routes; direct mixing of silica and titania sols (sample labeled as HB), cohydrolysis−condensation of acac-stabilized Ti and Si precursors (sample labeled as Co-A), and cohydrolysis−condensation of acac-stabilized Ti and activated Si precursors (sample labeled as Co−B). The activated-Si precursor was prepared by partially hydrolyzing TEOS with a molar ratio of TEOS to water at 1:1. Sample HB was prepared by mixing titania with silica sols, which were first prepared by adding water into Ti and Si precursors separately. Sample Co-A was prepared by adding water into the mixture of acac-stabilized Ti and Si precursors and sample Co−B was prepared by adding water into the mixture of acac-stabilized Ti and activated-Si precursors. All of the above samples were aged at room temperature and then coated on glass slide (for observation), quartz substrate (for optical test), Si substrate (for composition analysis), and Al-deposited Si wafer (for compositional depth profile analysis) by a spincoater with a spin rate of 1000 to 2000 rpm. The thicknesses of the samples estimated by ellipsometry were 500 to 700 nm. The films were annealed at 180 °C for 1 h in ambient atmosphere.

All optical measurements were performed by comparing samples on a substrate without coating. Optical absorption of the films was recorded by UV−vis−IR spectrophotometry. The optical constants of samples were obtained by ellipsometry. The optical constants of sample Co-A were measured by a point-to-point fitting, while those of HB and Co−B were extracted from the simulated curve using effective medium approximation (EMA) since the point-to-point method failed to fit the data. The chemical composition and stoichiometry of the samples were studied by X-ray photoelectron spectroscopy (XPS, Ulvac-PHI PHI 1600) with Mg K_α (1253.6 eV) and a spot size of ~2 × 2 mm. The anode voltage was kept at 15.0 kV the detection angle was 54°. The carbon signal (C 1s = 284.5 eV) was used as a reference to eliminate possible shift of the equipment and charging of samples.[19] The raw data were smoothed to reduce the noise of instrument origin and corrected by a blend of a linear and Shirley backgrounds in an iterative determination.[20−22] Deconvolution of the XPS data was performed by using Gaussian function with 1 to 10 curves to regenerate fit curves. As the XPS data in the present study are relatively symmetric, introduction of asymmetric functions such as Voigt does not have a better fit of the experimental data (Supporting Information). All fittings were not converged while using more than three Gaussian curves. For HB, three Gaussian functions generate a robust result with R^2 = 0.99976. For Co-A and Co-B, instead, two Gaussian functions produce more robust curves than single Gaussian function (R^2 = 0.99848 and 0.99941, respectively). The compositional depth profile was analyzed by Auger electron spectroscopy (AES, Ulvac-PHI PHI 700) with 5 keV electron beam (diameter of the spot size ~50 μm). Neglecting some of the near-surface and near-substrate areas, variation of atomic contents in the out-of-plane orientation of the whole film was estimated.

3. RESULTS AND DISCUSSION

3.1. Preparation of Silica−Titania Films. Silica−titania thin film can be simply prepared by mixing silica and titania sols, as shown in Figure 1a. One of the advantages of the direct

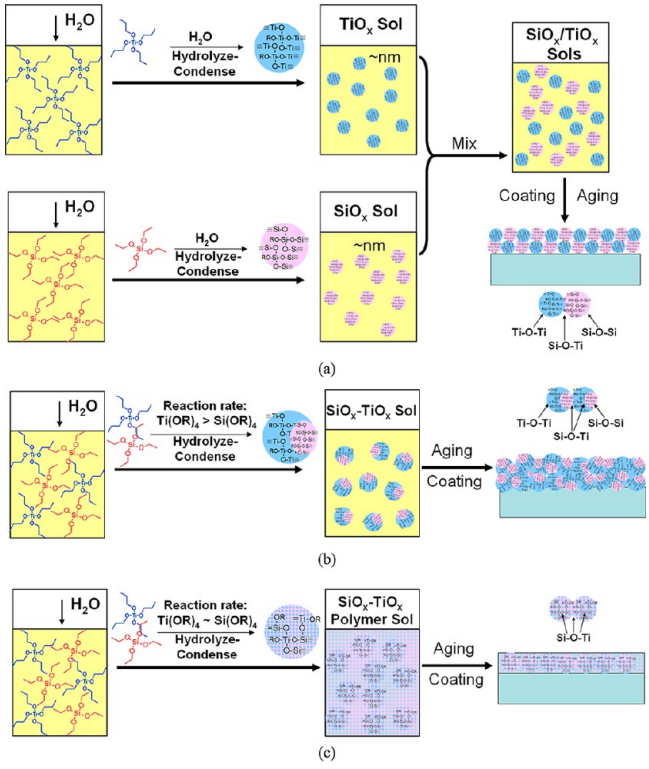

Figure 1. Illustration of three sol−gel processes to form silica−titania films. (a) SiO_x and TiO_x sols prepared separately (process for HB). (b) TEOS and TTIP are cohydrolyzed (process for Co-A). TTIP has a higher hydrolysis rate than TEOS. (c) Co-hydrolysis of TEOS and TTIP (process for Co-B). Both have similar hydrolysis rates.

mixing method is that silica and titania can be prepared separately with their optimum experimental conditions, avoiding a large difference in the reaction kinetics between Si and Ti alkoxides. In this case, the homogeneity of the hybrid film is dependent on the dimension and the functionality of the titania and silica sol particles. The smaller the sol particles prepared, the less compositional and structural fluctuations in the mixed sols and thus a more homogeneous film can be obtained. The functionality of the sol particles determined by the acidity and the amount of water can affect adhesion of the sol particles. For Si alkoxides, which have a very slow reaction rate with water (~hours to days), their hydrolysis needs to be catalyzed in an acidic or basic condition to speed up the reaction. In an acidic condition, the hydrolysis rate is faster than the condensation rate so smaller sol particles and gel network

dx.doi.org/10.1021/am301113a | ACS Appl. Mater. Interfaces 2012, 4, 5188−5195

will form. Moreover, Si alkoxides are not miscible with water, so the phase separation will occur during the hydrolysis−condensation process. Thus, Si alkoxides are typically mixed with ethanol to improve their dispersion in water. On the other hand, it is more difficult to control titania size and morphology in the sol−gel process because Ti alkoxides such as TTIP rapidly react with water (~seconds), leading to large precipitates in a solution. Therefore, preparation of silica−titania composite materials by separately synthesizing silica and titania sols could largely reduce the process complexity. But the homogeneity of the composite from this approach may be limited by the size of the sol particles. The film HB was prepared in accordance with this process.

Intuitionally, the hydrolysis−condensation reaction of Si and Ti alkoxides may be performed at the same time to improve the molecular homogeneity. TEOS and TTIP, i.e., $Si(OC_2H_5)_4$ and $Ti(OC_3H_7)_4$, respectively, are miscible to each other, so they would be suitable to carry out the cohydrolysis−condensation or copolymerization. However, addition of water into a $Si(OC_2H_5)_4/Ti(OC_3H_7)_4$ mixture may simply lead to formation and segregation of large inhomogeneous titania ~~sol~~ particles because the hydrolysis−condensation rate of TTIP is known to be much faster than that of $Si(OC_2H_5)_4$, as schematically shown in Figure 1b. This is the process adopted to prepare the Co-A film. Consequently, control over the reactions of both $Ti(OC_3H_7)_4$ and $Si(OC_2H_5)_4$ with water is a key issue to deal with the cohydrolysis−condensation of the mixed alkoxides. If the reactivity of $Ti(OC_3H_7)_4$ with water is comparable to that of $Si(OC_2H_5)_4$, the hydrolysis−condensations of both alkoxides are able to carry out simultaneously and molecularly heterometal Ti−O−Si bonds can form in the reaction process, as shown in Figure 1c. This is the process to prepare the Co-B film.

HB, Co-A, and Co-B samples were prepared using the same formula but with different reaction routes. The HB film was prepared by mixing silica sols with titania sols, which were separately synthesized from $Si(OC_2H_5)_4$ and acac-stabilized $Ti(OC_3H_7)_4$. The hydrolysis of pure $Ti(OC_3H_7)_4$ was very fast, so it was first stabilized by acac. Introduction of equal molar acac to $Ti(OC_3H_7)_4$ resulted in a chelated titanate compound acac-$Ti(OC_3H_7)_4$, which had a clear yellowish color and was stable in ambient atmosphere for hours. The hydrolysis of acac-Ti-$(OC_3H_7)_4$ mainly causes -(OC_3H_7) ligands to be replaced by −OH ones and Ti coordination number to increase from four to five.[23] Without the stabilizer, addition of water would rapidly result in precipitation of large white particles. The aging time of the Ti and Si sols was about 1−3 h before they were mixed with each other. Longer aging time can cause larger sol or gel particles that may decrease the homogeneity of the hybrid. On the other hand, the Co-B film was prepared from activated $Si(OC_2H_5)_4$ and acac-stabilized $Ti(OC_3H_7)_4$. In the synthetic process, the amount of water was divided into two parts; a portion of water was used to activate $Si(OC_2H_5)_4$ (with equal moles) and the rest amount of water was then used to perform the cohydrolysis−condensation of the mixture of Si and Ti alkoxides. Premixing of equal moles of water and $Si(OC_2H_5)_4$ produces $(OC_2H_5)_3Si-OH$,[8] which is more reactive than $Si(OC_2H_5)_4$. The prehydrolyzed $(OC_2H_5)_3Si-OH$ can react with $Ti(OC_3H_7)_4$ and preferentially forms heterometal oxides bond Si−O−Ti.[8] It has been shown that the postaddition of water to promote condensation of Ti-OR could prevent a partial cleavage of the Si−O−Ti bonds in solution for titanium n-butoxide.[16] Addition of the rest amount of water into the mixture of $(OC_2H_5)_3Si-OH$ and acac-$Ti(OC_3H_7)_4$ could cause fast hydrolysis/condensation of acac-$Ti(OC_3H_7)_4$, leading to reactive acac-$Ti(OC_3H_7)_3(OH)$ and initiate the condensation on Si-OC_2H_5 moieties. The reactions finally result in transparent viscous gels.

3.2. Optical Absorption. Figure 2a presents the transmittance spectra of HB, Co-A, and Co−B together with a solar

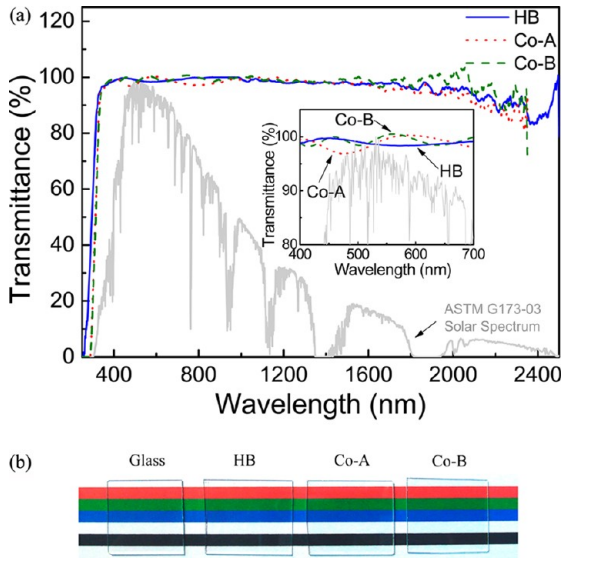

Figure 2. (a) Transmittance spectra of silica−titania thin films; HB (thickness = 620 nm), Co-A (thickness = 655 nm), and Co−B (thickness = 670 nm) spin-coated on glass substrates. A solar spectrum (ASTM G173−03) is plotted for reference. The inset shows transmittance spectra in the short wavelength range. (b) Photos of the samples and an uncoated glass reference placed on a sheet of paper printed with red, green, blue, and black color strips.

spectrum (ASTM G173−03) plotted for reference. The transmittances of all samples in the range of 350−1800 nm are more than 97%. The transmittance of HB is higher in the UV range (inset) but lower in the range of 550−650 nm compared with Co-A and Co-B. Co-A shows less transparency in the ranges of 450−520 nm and 700−1000 nm and Co−B shows the highest transparency among the samples. Figure 2b displays a photo of the samples coated on glass slides placed on a sheet of paper.

The refractive index of Co−B was measured by point-by-point fitting without approximation, while the indices of both HB and Co-A were obtained using the effective medium approximation. The refractive indices of TiO_2 and SiO_2 are 2.52 and 1.46, respectively.[24] The refractive index of the film may not be simply calculated by the linear interpolation between TiO_2 and SiO_2 since the sol−gel-derived thin films may not be completely homogeneous (will be shown below). The ellipsometric measurement is capable of gaining the refractive index as a function of wavelength. As shown in Figure 3, the indices of HB and Co-A samples at 300−1100 nm are 1.86−1.60 (1.64 at 500 nm) and 1.88−1.60 (1.65 at 500 nm), respectively, that decrease with wavelength known as dispersion. For Co−B at 300−1100 nm, the index is 1.79−1.59 (1.62 at 500 nm). The refractive index is strongly affected by the composition and microstructure of thin films. For example, the index value increases with increasing Ti-component percentage in silica−titania thin films prepared by PECVD.[25] The compositional profiles, microstructures, and

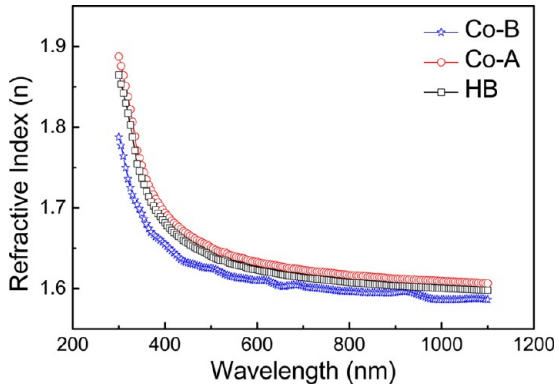

Figure 3. Refractive indices of HB, Co-A, and Co-B. The indices of HB and Co-A are obtained using the effective medium approximation and that of Co-B is extracted from point-by-point fitted curve.

dimension of silica, titania, and their interface (i.e., Si−O−Ti) domains can largely affect the optical properties of the silica−titania thin films. A detail study in the optical properties of the films will be published elsewhere.

3.3. SEM and XRD. X-ray diffraction (XRD) patterns of all samples show a broad peak at around $2\theta = 20°$, indicating that the samples are amorphous or less crystalline (Supporting Information). Figure 4 shows the scanning electron microscopic (SEM) images of HB (a), Co-A (b), and Co−B (c). All samples display a dense and smooth morphology. No primary and secondary particles are observed. The insets in (b) and (c) are taken from the edges of the samples.

3.4. X-ray Photoelectron Spectra. Figure 5a shows full-range XPS spectra of HB, Co-A, and Co−B thin solid films, which display that Si, Ti, and O peaks with chemical shifts are present in all samples. The reported binding energies of Ti $2p^{3/2}$ and Si $2p^{3/2}$ are 454.0 and 99.5 eV, respectively.[26,27] The chemical shift is dependent not only on the energy level of electrons but also on the local environment of the atoms that causes variation of strength of the chemical bonding. For example, increase in the oxidation state results in a stronger Columbic interaction between the electrons and the core and therefore the binding energy shifts to the higher energy side. Figure 5b shows that the Si $2p^{3/2}$ binding energies of HB, Co-A, and Co-B are 102.8, 102.8, and 102.2 eV, respectively. The electronic binding energies at $2p^{3/2}$ in Si of all samples are lower than that in pure SiO_2 (104.0 eV),[28] indicating the Si atoms in the samples are less affected by electronegative species (i.e., O atoms) compared with that in SiO_2, which may result in a intermediate oxdiation state between those in Si and SiO_2. The lower O content sensed by Si is attributed to either less O or variation of the local chemical environment of Si in the films.

The average O atomic contents of all samples are slightly less than two (from AES, will be shown later) so the Si $2p^{3/2}$ binding energies within the range of 99.5−104.0 eV are expected. However, it is noted that Co−B has a smaller Si $2p^{3/2}$ binding energy compared with the other two, which is not caused by the O content since Co-A has less oxygen than Co−B from AES analysis. This result might be caused by a variation of local environment of Si that makes electrons in Si $2p^{3/2}$ change their binding energy. The difference in the local environment of Si in Co−B may be assigned to a local fluctuation of the chemical composition around Si that relates to the homogeneity. Moreover, the film homogeneity is determined by the dimensions of SiO_x and TiO_x domains,

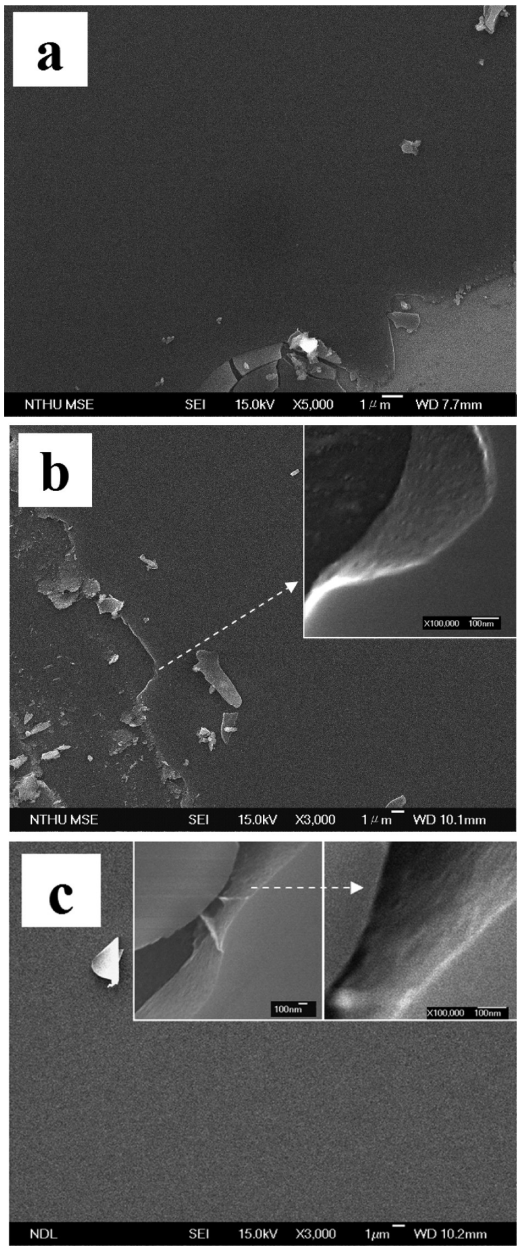

Figure 4. SEM images of silica−titania thin films; (a) HB, (b) Co-A, and (c) Co-B. The inset images in b and c are taken from the edges of the samples.

which are silica and titania clusters respectively, or building blocks of SiO_4 tetrahedrons and TiO_6 octahedrons respectivley. A film with smaller silica and titania domains having more domain boundaries is more homogeneous. As the Si−O−Ti bond bridges silica and titania matrice (domains) that exists in the interface region (i.e., boundaries), the Si−O−Ti content in the film relates to the homogeneity. Therefore, the film homogeneity is in connection with the Si−O−Ti content and the core electron binding energies of the atoms. In a hybridized silica−titania film, the SiO_x or TiO_x domains can retard the growth of large domains of the other, that is, the domains of the SiO_4 tetrahedrons can be cleaved by insertions of titania units such as TiO_6 octahedrons and vice versa. When the SiO_x domain size decreases, more domain boundaries exist because the orientation and the edge length of SiO_4 tetrahedrons very differ from those of TiO_6 octahedrons. The domain boundary

dx.doi.org/10.1021/am301113a | ACS Appl. Mater. Interfaces 2012, 4, 5188−5195

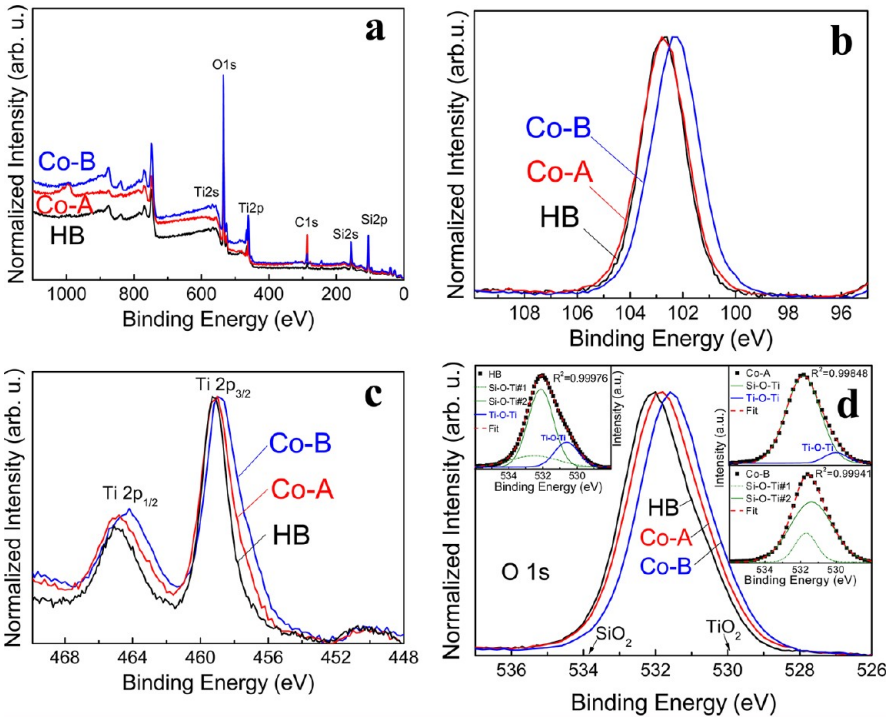

Figure 5. (a) X-ray photoelectron spectra of silica−titania films. The binding energies of (b) Si $2p^{3/2}$, (c)Ti 2p, and (d) O 1s. The insets in d show the deconvoluted curves for each of the three samples.

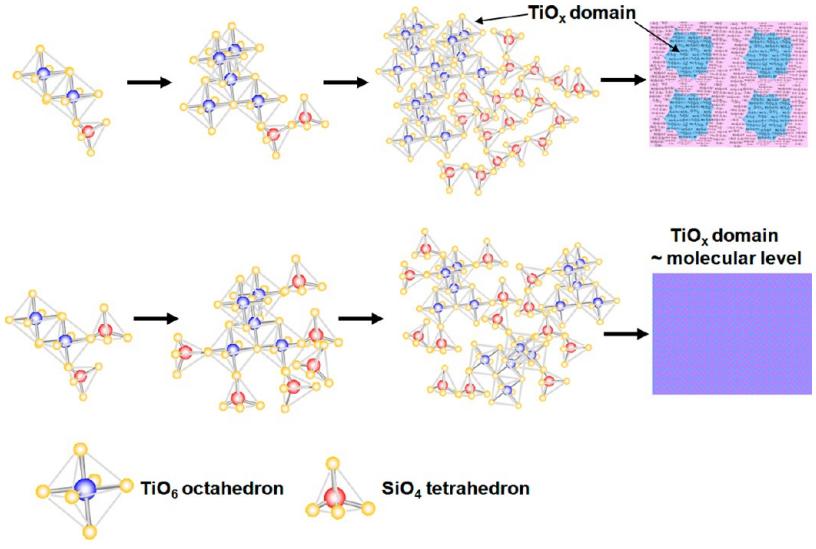

Figure 6. Sketches of the structures of silica−titania films with lower (top) and higher (bottom) degrees of hybridization of the SiO_4 tetrahedrons and TiO_6 octahedrons. The molecular bond length and atomic size are not to scale. The connection between TiO_6 octahedrons is based on the edge-sharing. TiO_4 tetrahedron is not included in the sketches.

region is a highly disordered structure, in which the ratio of O to metal ions is substoichiometric (i.e., $x < 2$ for SiO_x), so Si $2p^{3/2}$ electron in such reion would possess a smaller binding energy compared with that in larger domains, in which are SiO_2, in nonhomogeneous films. Similar situation is found in Ti $2p^{3/2}$ XPS spectra, as shown in Figure 5c. A shoulder appears at the lower energy side of the peak, indicating a portion of Ti atoms in Co−B are affected by less O because of the more domain boundaries (i.e., $x < 2$ for TiO_x). A higher degree of hybridization of TiO_x and SiO_x in Co−B sample is ascribed to a comparable reaction rate of Si to that of Ti alkoxides in the hydrolysis−condensation. In this situation, SiO_4 tetrahedrons have a higher probability of connecting TiO_6 octahedrons and could retard the connection of TiO_6 octahedrons themselves into a larger cluster so a more disordered structure could be created.

Figure 5d displays the O 1s spectra of the samples. The O 1s binding energies of the HB, Co-A, and Co−B are 532.1, 531.8, and 531.5 eV, respectively. Deconvolution shows that the O 1s peak of HB is composed of three subpeaks at 532.5, 532.1, and 530.3 eV. The O 1s of pure reference SiO_2 and TiO_2 are 533.7 and 529.9 eV, respectively. The O 1s in Si−O−Ti bond has been proposed to have a binding energy between those in the Si−O−Si and Ti−O−Ti ones.[29] As Ti are less electronegative

dx.doi.org/10.1021/am301113a | ACS Appl. Mater. Interfaces 2012, 4, 5188−5195

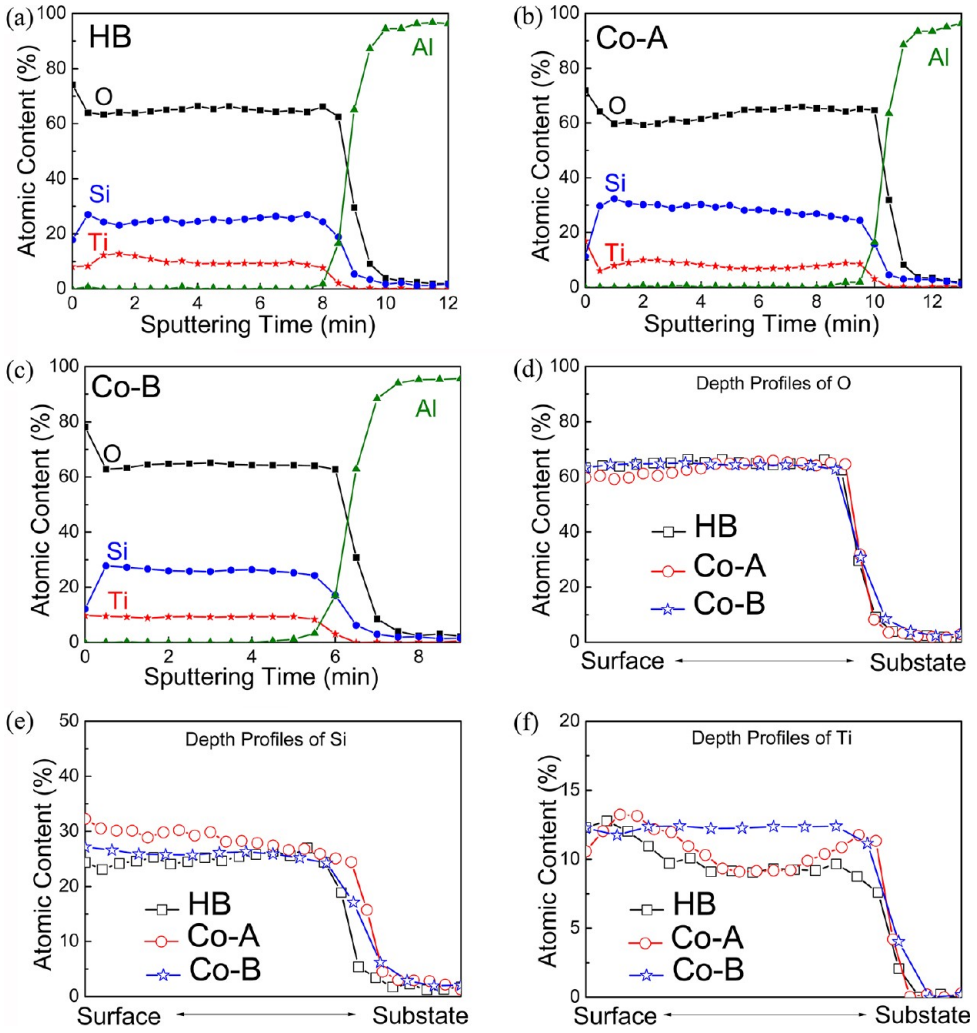

Figure 7. Auger depth profiles of elemental O, Si, and Ti in silica–titania thin films. (a) HB, (b) Co-A, and (c) Co-B. The samples are coated on Al-deposited Si substrate. The depth profiles of the elements for three samples are replotted in d–f for comparsion.

than Si (Pauling values Ti ~ 1.5 and Si ~ 1.8), the O 1s core electron binding energy decreases when a Si–O–Si bond is replaced by a Ti–O–Si bond.[30] Therefore, both of 532.5 and 532.1 eV peaks are assigned to the Si–O–Ti bonds, while the 530.3 eV peak is related to the Ti–O–Ti bonds from TiO_2. For Co-A, the O 1s spectrum consists of two subpeaks at 531.8 and 530.0 eV, arisen from Si–O–Ti and Ti–O–Ti bonds, respectively. Decomposition of the XPS data of Co–B only generates two subpeaks at 531.4 and 531.6 eV, both of which are attributed to the Si–O–Ti bonds. The deconvolution result shows that the Co–B curve has a larger proportion in the Si–O–Ti region, which supports that Co–B has a relatively higher molecular homogeneity than the other two samples (see Supporting Information). The metal hydroxide bonding would not be predominant in the thin films as Si–OH or Ti–OH reacts with themselves easily via removal of water in the sol–gel polycondensation process. They are chemically less stable compared with the metal oxide bonds. In addition, the surfaces of the samples were etched by Ar ion bream before the measurements were carried out. The deconvoluted curves appear to show that certain mixing modes of titania and silica units, e.g., TiO_6 octahedrons and SiO_4 tetrahedrons, might exist in silica–titania thin films, which is still under investigation.

Figure 6 schematically shows the hybridization of silica and titania units in the case of SiO_4 tetrahedrons and TiO_6 octahedrons. The Si–O–Ti bond acts as the connection between SiO_4 tetrahedrons and TiO_6 octahedrons. The inhomogeneity of the samples could be caused by the inconsistent reaction rate between the Ti and Si precursor compounds. If the hydrolysis–condensation of Ti compounds is faster than that of Si ones, TiO_6 octahedrons tend to be clustered rather than being connected with the dissimilar SiO_4 tetrahedrons, as shown in Figure 6 (top). If they have similar reactivity, a higher degree of hybridization of silica and titania can be achieved and the resulted hybrid film could be in molecular level hybridization.

3.5. Auger Depth Profile. The XPS provides in-plane compositional information on the film surface, while AES depth profile provides out-of-plane compositional data in the film. Figure 7 presents the compositional depth profiles of the samples. Al signal is used to mark the position of the substrates. The O, Si, and Ti populations show no significant variations in all samples. The Ti/Si ratios at the middle depth of HB, Co-A, and Co-B samples are 0.36, 0.24, and 0.35, respectively. A comparison of the atomic contents among the samples is made in Figure 7d–f. The O and Si contents are roughly stable in all samples, while the Ti content fluctuates in them except Co-B.

dx.doi.org/10.1021/am301113a | ACS Appl. Mater. Interfaces 2012, 4, 5188–5195

The average atomic contents of O, Si and Ti estimated from AES depth profiles in the HB film are 65.07, 25.05, and 9.77 with the standard deviations (SD) of 1.20, 2.90, and 9.58%, respectively. Obviously, the distribution of Ti is not even in the out-of-plane orientation in the HB sample. This result would be due to higher reactivity of the surface of the titania sol particles compared with that of the silica sol particles. As a result, the coalescence of the titania sol particles is spontaneously fast and those bigger aggregates are separated in the coating and drying process. Unfortunately, it is hard to avoid this situation if the reactivity of hydrolyzed Ti compound is high.

Co-A was prepared by cohydrolysis−condensation of premixed solution of $Si(OC_2H_5)_4$ and acac-stabilized Ti-$(OC_3H_7)_4$ but it did not show a better homogeneity than HB. The Ti content still has a large out-of-plane fluctuation in the Co-A film, while Si content also gradually decreases when approaching to the substrate (Figure 7). The average atomic contents of O, Si, and Ti in the Co-A film are estimated to be 63.04 ± 3.74%, 28.75 ± 4.50%, and 7.97 ± 14.49%, respectively. It is noted that the standard deviations of both Si and Ti contents in Co-A are higher than those in HB, indicating that larger titania clusters and/or sol particles are present in the film. Compared with HB, the deviation values of the composition of Co-A are larger by 67.90%, 35.50%, and 33.80% for O, Si, and Ti, respectively. Note that the increases in the deviations values of the Si and Ti atomic contents in Co-A are comparable. Moreover, the shapes of the depth profiles in Co-A resemble to those of HB (Figure 7). The results might be due to a similar formation process for Co-A to that for HB, that is, larger titania domains form because of a faster reaction rate of Ti alkoxide that causes the heterogeneity of Co-A. Those larger titania particles cause vertical inhomogeneity during the thin film formation process that involves spin-coating and drying, where applied centrifugal force and evaporation of solvents from the wet films cause redistribution of the titania particles in the out-of-plane direction. The out-of-plane inhomogeneity would be inevitable if the in-plane inhomogeneity exists. The in-plane homogeneity, on the other hand, is mainly determined by the larger titania clusters forming in the reaction process.

The average atomic contents of O, Si, and Ti in Co-B estimated from AES, on the other hand, are 64.61 ± 0.48%, 25.87 ± 1.36%, and 9.26 ± 0.57%, respectively. All the deviations of O, Si, and Ti atomic contents are less than 1.5% along the out-of-plane orientation throughout the film (∼ 700 nm), showing an excellent homogeneity. Combined the AES result with that from XPS, it is concluded that Co−B is highly homogeneous in both in-plane and out-of-plane orientations. The high homogeneity is responsible for the excellent optical transparancy of the films.

All of the thin solid films are substoichiometric. The ratios of O/(Si+Ti) of HB, Co-A, and Co−B samples are 1.87, 1.72, and 1.84, respectively. This is because the amorphous thin solid films are in the glassy state and has a highly disordered structure. Unlike silica−titania hybrid particles prepared by precipitation or evaporation of solvents, the coating and annealing in the thin film processing strongly affects the construction of silica−titania hybrid. The differences in the orientation and the edge length between the SiO_4 tetrahedrons and the TiO_6 octahedrons can lead to domain boundaries and nonstoichiometry for silica−titania materials in the solid state. Moreover, it is noted that the oxygen substoichiometry content is not connected to the degree of homogeneity, i.e., the most homogeneous sample (Co−B) is not correspondent with the lowest ratio of O/(Si+Ti). We suggest that a certain mixing mode or configuration of silica and titania units (e.g., SiO_4 tetrahedrons and TiO_6 octahedrons) exists in the amorphous silica−titania thin solid film.

4. CONCLUSION

Transparent silica−titania thin films with a thickness of 500−700 nm were synthesized by three different sol−gel paths, i.e. mixing of silica and titania sols (HB), cohydrolysis−condensation of mixed Si and acac-stabilized Ti alkoxides (Co-A), and cohydrolysis−condensation of OH-activated Si and acac-stabilized Ti alkoxides (Co-B). All films are highly transparent and have the transmittance more than 97% in the range of 350−1800 nm. X-ray photoelectron spectroscopy demonstrates that the third path leads to the best molecularly homogeneous silica−titania film due to comparable reactivity. The deviations of O, Si, and Ti atomic contents of the Co-B film in both in-plane and out-of-plane (∼700 nm) orientations are all less than 1.5%.

■ ASSOCIATED CONTENT

Ⓢ Supporting Information

This material is available free of charge via the Internet at http://pubs.acs.org.

■ AUTHOR INFORMATION

Corresponding Author

*E-mail: sean.chen@cantab.net (H.-S.C.); tpperng@mx.nthu.edu.tw (T.-P.P.).

Notes

The authors declare no competing financial interest.

■ ACKNOWLEDGMENTS

This work was supported by the National Science Council of Taiwan under Contract NSC-99-2221-E-007-066-MY. The authors acknowledge valuable discussion on XPS data with Prof. Chi-Young Lee and thank Mr. Su-Jin Hsiao and Mr. Kuo-Wei Wu in Prof. Lih-Hsin Chou's lab, and Mr. Chang-Wen Chen in Prof. Hao-Wu Lin's lab in NTHU for XRD and optical spectral measurements.

■ REFERENCES

(1) Chen, H. S.; Kumar, R. V.; Glowacki, B. A. *J. Sol−Gel Sci. Technol.* **2009**, *51*, 102.
(2) Seo, J. Y.; Han, M. *Nanotechnology* **2011**, *22*, 025601.
(3) Xu, Y.; Zhang, B.; Fan, W. H.; Wu, D.; Sun, Y. H. *Thin Solid Films* **2003**, *440*, 180.
(4) Gerritsen, M.; Kros, A.; Sprakel, V.; Lutterman, J. A.; Nolte, R. J.; Jansen, J. A. *Biomaterials* **2000**, *21*, 71.
(5) Olding, T.; Sayer, M.; Barrow, D. *Thin Solid Films* **2011**, *398−399*, 581.
(6) Anderson, C.; Bard., A. J. *J. Phys. Chem.* **1995**, *99*, 9882.
(7) Liu, J.; Shi, F.; Yang, D. *J. Mater. Sci. Technol.* **2004**, *20*, 550.
(8) Yoldas, B. E. *J. Non-Cryst. Solids* **1980**, *38&39*, 81.
(9) Jung, M. *Int. Inorg. Mater* **2001**, *3*, 471.
(10) Yamane, M.; Inoue, S.; Nakazawa, K. *J. Non-Cryst. Solids* **1982**, *48*, 153.
(11) Andrianainarivelo, M.; Corriu, R.; Leclercq, D.; Mutin, P. H.; Vioux, A. *J. Mater. Chem.* **1996**, *6*, 1665.
(12) Lin, C. C.; Basil, J. D. *Mater. Res. Soc. Symp. Proc.* **1986**, *73*, 173.
(13) Basil, J. D.; Lin, C. C. *Mater. Res. Soc. Symp. Proc.* **1988**, *121*, 49.
(14) Hoebbel, D.; Reinert, T.; Schmidt, H. *J. Sol−Gel Sci. Technol.* **1996**, *6*, 139.

(15) Hoebbel, D.; Nacken, M.; Schmidt, H. *J. Sol–Gel Sci. Technol.* **1998**, *13*, 37.
(16) Babonneau, F.; Delattre, L. *Chem. Mater.* **1997**, *9*, 2385.
(17) Crouzet, L.; Leclercq, D.; Mutin, P. H.; Vioux, A. *Chem. Mater.* **2003**, *15*, 1530.
(18) Chen, H. S.; Kumar, R. V.; Glowacki, B. A. *Mater. Chem. Phys.* **2010**, *122*, 305.
(19) Smith, K. L.; Black, K. M. *J. Vac. Sci. Technol., A* **1984**, *2*, 744.
(20) Shirley, D. A. *Phys. Rev. B* **1972**, *5*, 4709.
(21) Anderson, O. *Vacuum* **1990**, *41*, 1700.
(22) Paparazzo, E. *J. Electron Spectrosc. Relat. Phenom.* **2006**, *154*, 38.
(23) Babonneau, F.; Sanchez, C.; Livage, J. *J. Non-Cryst. Solid* **1988**, *106*, 170.
(24) Exarhos, G. J.; Pawlewicz, W. T. *Appl. Opt.* **1984**, *23*, 1986.
(25) Gracia, F.; Yubero, F.; Holgado, J. P.; Espinos, J. P.; Gonzalez-Elipe, A. R.; Girardeau, T. *Thin Solid Films* **2006**, *500*, 19–26.
(26) Ermolieff, A.; Bernard, P.; Marthon, S.; Wittmer, P. *Surf. Interface Anal.* **1988**, *11*, 563.
(27) Wittmer, M.; Oelhafen, P.; Tu, K. N. *Phys. Rev. B* **1986**, *33*, 5391.
(28) Bell, F. G.; Ley, L. *Phys. Rev. B* **1988**, *37*, 8383.
(29) Ingo, G. M.; Dire, S.; Babonneau, F. *Appl. Surf. Sci.* **1993**, *70*, 230.
(30) Reddy, B. M.; Chowdhury, B.; Smirniotis, P. G. *Appl. Catal. A* **2001**, *211*, 19.